# A model describing flowback chemistry changes with time after Marcellus Shale hydraulic fracturing

**Victor N. Balashov, Terry Engelder, Xin Gu, Matthew S. Fantle, and Susan L. Brantley**

## ABSTRACT

Between 2005 and 2014 in Pennsylvania, about 4000 Marcellus wells were drilled horizontally and hydraulically fractured for natural gas. During the flowback period after hydrofracturing, 2 to $4 \times 10^3$ m$^3$ (7 to $14 \times 10^4$ ft$^3$) of brine returned to the surface from each horizontal well. This Na-Ca-Cl brine also contains minor radioactive elements, organic compounds, and metals such as Ba and Sr, and cannot by law be discharged untreated into surface waters. The salts increase in concentration to ~270 kg/m$^3$ (~16.9 lb/ft$^3$) in later flowback. To develop economic methods of brine disposal, the provenance of brine salts must be understood. Flowback volume generally corresponds to ~10% to 20% of the injected water. Apparently, the remaining water imbibes into the shale. A mass balance calculation can explain all the salt in the flowback if 2% by volume of the shale initially contains water as capillary-bound or free Appalachian brine. In that case, only 0.1%–0.2% of the brine salt in the shale accessed by one well need be mobilized. Changing salt concentration in flowback can be explained using a model that describes diffusion of salt from brine into millimeter-wide hydrofractures spaced 1 per m (0.3 per ft) that are initially filled by dilute injection water. Although the production lifetimes of Marcellus wells remain unknown, the model predicts that brines will be produced and reach 80% of concentration of initial brines after ~1 yr. Better understanding of this diffusion could (1) provide better long-term planning for brine disposal; and (2) constrain how the hydrofractures interact with the low-permeability shale matrix.

### AUTHORS

VICTOR N. BALASHOV ~ *Earth and Environmental Systems Institute, 2217 EES Building, Pennsylvania State University, University Park, Pennsylvania 16802; vnb1@psu.edu*

Victor N. Balashov is a research associate in the Earth and Environmental Systems Institute at the Pennsylvania State University (Penn State) since 2010. Between 1973 and 2000, he served in positions from graduate research assistant to senior research scientist at the Institute of Experimental Mineralogy (Russian Academy of Science). He earned a B.S. degree in chemistry from Lomonosov Moscow State University (Russia), and a Ph.D. in chemistry from Vernadskii Institute of Geochemistry and Analytical Chemistry, Russian Academy of Science.

TERRY ENGELDER ~ *Dept. of Geosciences, Pennsylvania State University, University Park, Pennsylvania 16802; jte2@ems.psu.edu*

Terry Engelder has served as professor of geosciences in the Department of Geosciences at Penn State since 1985. Before that, he served at the Lamont-Doherty Earth Observatory, the US Geological Survey, and Texaco. He earned a B.S. degree in geology from Penn State, an M.S. degree in geology from Yale University, and a Ph.D. in geology from Texas A&M University.

XIN GU ~ *Dept. of Geosciences, Pennsylvania State University, University Park, Pennsylvania 16802; xug102@psu.edu*

Xin Gu is a Ph.D. student in the Department of Geoscience at Penn State. He earned a B.S. degree from Tsinghua University (China), and an M.S. degree from Penn State. His current research interests are characterization of pore structures and weathering profiles of shale.

MATTHEW S. FANTLE ~ *Earth and Environmental Systems Institute, 2217 EES Building, Pennsylvania State University, University Park, Pennsylvania 16802; Dept. of Geosciences, Pennsylvania State University, University Park, Pennsylvania 16802; msf17@psu.edu*

Matthew S. Fantle is an assistant professor of geosciences at Penn State. He serves as the director of the Metal Isotope Laboratory at Penn State, which houses a Thermo Scientific Neptune Plus MC-ICP-MS. Prior to joining the Penn State faculty in 2006, he received a B.A. degree from Dartmouth College and a Ph.D. in geology from the University of California, Berkeley.

SUSAN L. BRANTLEY ~ *Earth and Environmental Systems Institute, 2217 EES Building,*

*Pennsylvania State University, University Park, Pennsylvania 16802; Dept. of Geosciences, Pennsylvania State University, University Park, Pennsylvania 16802; sxb7@psu.edu*

Susan Brantley is distinguished professor of geosciences in the Department of Geosciences at Penn State. She joined the faculty at Penn State in 1986. Before that, she earned an A.B., M.S. and a Ph.D. in geological and geophysical sciences from Princeton University. She has published more than 160 papers on aspects of water–rock interaction.

### DATASHARE 58

Tables S1, S2, S3, Figures S1, S2, S3 are available in an electronic version on the AAPG website (www.aapg.org/datashare) as Datashare 58.

### EDITOR'S NOTE

A color version of Figure 1 can be seen in the online version of this paper.

## INTRODUCTION

Horizontal drilling and large-volume hydraulic fracturing (i.e., hydrofracturing) is now enabling production of natural gas from unconventional shale-gas plays in the United States, including the Barnett and Marcellus (Harper, 2008; Engelder, 2009; MIT, 2011). Globally, shale-gas reservoirs are abundant, and these techniques may soon be used worldwide (MIT, 2011). However, in the Middle Devonian Marcellus Shale of the Hamilton Group, significant concerns have arisen about potential environmental effects (Entrekin et al., 2011; Vidic et al., 2013; Brantley et al., 2014). During hydrofracturing, millions of gallons of water are pumped into a well under pressure to open or create fractures in the shale (Nicot and Scanlon, 2012). After hydrofracturing, water returns to the wellhead (flowback), which is substantially saltier than the original injectate and is therefore costly to treat for disposal (Gregory et al., 2011; Maloney and Yoxtheimer, 2012). For example, each Marcellus well produces as much as 500,000–1,000,000 kg (551–1102 tons) of salt before gas production commences. In 2011 in Pennsylvania alone, almost 2.7 million $m^3$ (95 million $ft^3$) of salty flowback and production water were generated for the Marcellus play (Maloney and Yoxtheimer, 2012). Although much of the flowback water is now recycled in Pennsylvania for ongoing hydrofracturing, some of the waste was originally trucked to deep injection wells or, before 2011, discharged legally into streams (Maloney and Yoxtheimer, 2012; Olmstead et al., 2013). Eventually, once the rate of hydrofracturing decreases, the disposal of saline fluids will become an issue again (Vidic et al., 2013). We therefore need to understand the temporal evolution of the flow and chemistry of the brines.

Two major puzzles are related to the brines. First, less water returns to the surface than is injected (Nicot and Scanlon, 2012), and second, the flowback and production waters become increasingly saline with time (Figure 1). Although some have suggested that halite is present in the Marcellus Shale (Blauch et al., 2009), salt in flowback and production water more likely derives from Appalachian brine in the shale or surrounding formations (Rose and Dresel, 1990; Dresel and Rose, 2010; Haluszczak et al., 2012). In fact, data on naturally occurring radioactive materials (NORMs) (Rowan et al., 2011) and Sr isotopes (Osborn et al., 2011; Chapman et al., 2012) are consistent with flowback salts arising from brine in the Marcellus itself. However, well logs and other observations document little free water in the formation (Engelder, 2012; Engelder et al., 2014) and it has remained unclear as to whether enough salt is present in the shale to cause salinization of the returning water and just how that salinization
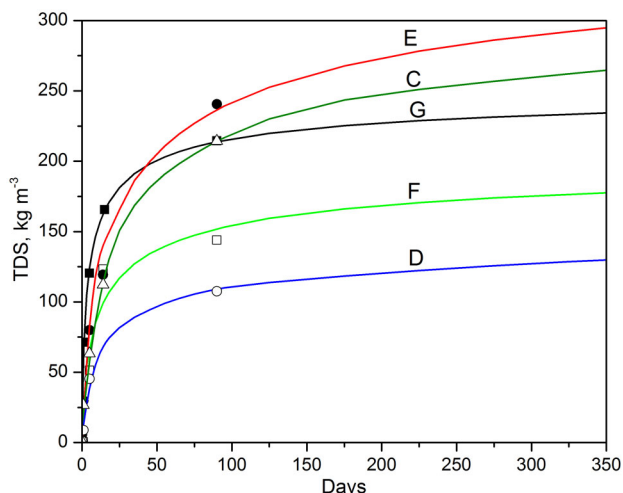
**Figure 1.** Plot showing how concentrations of total dissolved solids (TDS) changed with time in five horizontally drilled and hydrofractured wells (C, D, E, F, and G) (Hayes, 2009). Lines represent model output in which the values for the time rescaling coefficient ($b_1$) and the initial brine composition were fit to the data for each well (see text).

takes place. If brine is present, logs show that it must be in the form of water that is held by capillary forces, or very minor amounts of free water. Only the latter can drain out of the rock. Here, we investigate how much salt is present in Marcellus as brine and quantify how salt might enter flowback and production fluids. The model can also be used to predict average aperture of hydraulic fractures as a function of shale characteristics. Additionally, if the stimulated shale volume is known, then the spacing of hydraulic fractures can be predicted as well.

## BACKGROUND

Well logs from the Marcellus Shale show little water in the formation (Engelder et al., 2014). Commonly, only 1–2% of the shale volume contains water and most is capillary bound. An additional component of water is bound in the clay lattice. Data from >340 wells furthermore document that the Marcellus is only 23 ± 10% water saturated (Engelder, 2012). This means that only ~23% of the porosity (i.e., 0.23 × 0.01 to 0.02 of the shale volume) contains formation water (free or capillary bound), whereas the rest is filled by gas. Given this condition, a capillary seal can preclude water flow through the shale before

hydrofracturing (Engelder, 2012; Engelder et al., 2014). Brine is commonly found in rock units in the subsurface in the region underlain by Marcellus Shale (Poth, 1962; Rose and Dresel, 1990; Dresel and Rose, 2010; Haluszczak et al., 2012; Warner et al., 2012). Given the ubiquity of deep brine, we assume that where water is present in the Marcellus Shale, even as capillary-bound water, it is brine.

We propose a model in which the temporal increase of the salt concentration in flowback is explained by salt diffusion from capillary-bound or free brine in the shale matrix to the injectate water that fills fractures after hydrofracturing. This model is based on the assumption that salt diffuses out of matrix pores (diameters < 1 μm, as shown in pores of the shale documented in Figure 2, top) into fractures that are propped open after hydrofracturing by sand particles of diameter ≈ 500 μm (0.02 in.). Salt then is transported by flow into the borehole and returns to the surface as flowback. Pore connectivity inferred from neutron scattering (NS) of samples such as shown in Figure 2 (top) support this mechanism (Gu et al., 2014). For organic-rich shale core samples, NS data show that the total porosity can equal ~10.5% of the rock volume, whereas the connected porosity that can host water (termed here water-connected porosity) is ~3% of the rock volume. For four organic-poor shale samples from the same borehole sample shown in Figure 2 (top), the total porosity varied between ~5.3% and 7.1%, and the water-connected porosity between 1.3% and 2.4% (Gu et al., 2014). Therefore, in the proposed model the total porosity is set at 8.5%, and the water-connected porosity at 2%.

Although we have no images of hydrofractured shale because hydrofracturing generally occurs at depths of ~2000 m (~6560 ft) or deeper, in Figure 2 we show a sample of Marcellus Shale from an outcrop (Figure 2, bottom) that reveals an increase in porosity. Hydrofracturing occurs when the pressure of injectate exceeds the minimum confining stress in the rock above the rock tensile strength (Fjar et al., 2008). In contrast, the porosity increase in the shale (Figure 2, bottom) from an outcrop occurred because of exhumation rather than hydrofracturing. For this weathered shale, the pore data based on neutron scattering show the total porosity equals 16%, whereas
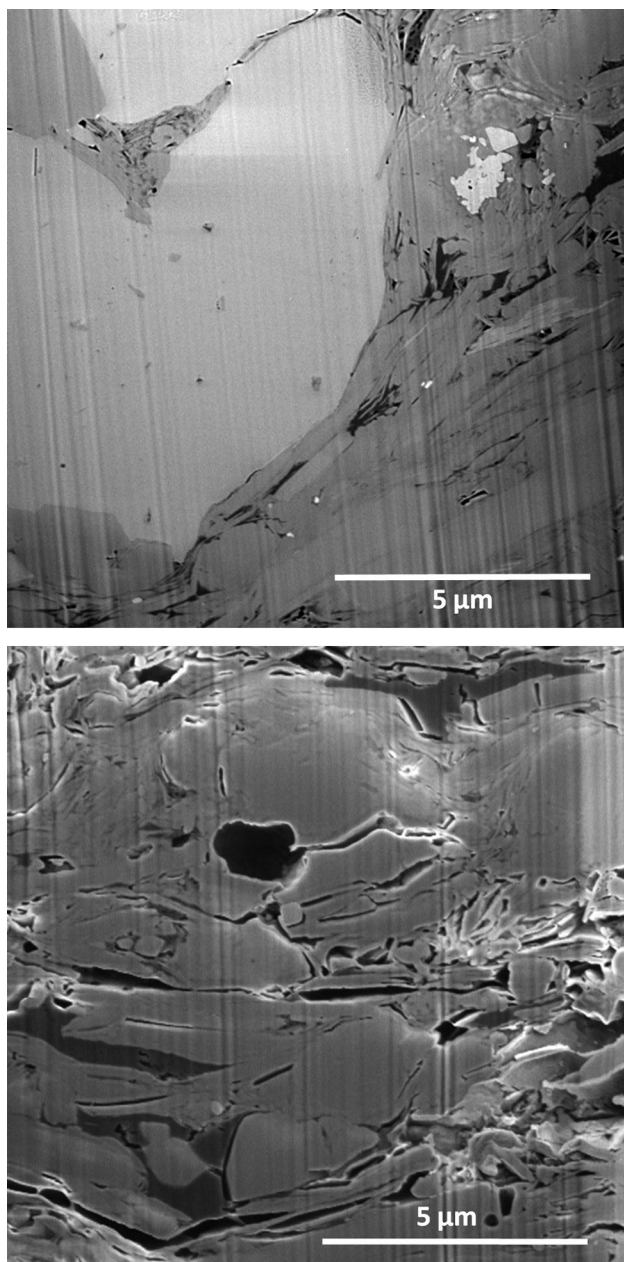
**Figure 2.** Backscattered scanning electron microscope (SEM) images of Marcellus Formation samples from 896 ft (273 m) below land surface (bls) from core from Howard, Pennsylvania (top), and from outcrop at a quarry near Frankstown, Pennsylvania (bottom, sampled from 31 ft [9.4 m] bls). The center part of the images have been field ion-beam (FIB) milled. Bright areas are denser than darker areas. Dark gray areas are organic matter and black areas are pores. Both sections were cut perpendicular to bedding (layer-like grains are clays lying along bedding). The bottom image, from a sample recovered from outcrop, shows higher porosity.

the water-connected porosity is 14.5% (Gu et al., 2014). By analogy, new porosity may result from hydrofracturing and may allow brine to diffuse from the shale matrix to the hydrofractures as subsequently discussed.

## BRINE AND ROCK CHEMICAL COMPOSITION

Rocks beneath Pennsylvania at depths greater than 500 to 1000 ft (152 to 305 m) often contain brine in interstitial pore fluids (Poth, 1962; Rose and Dresel, 1990; Warner et al., 2012). Here, we describe chemical evidence from two sets of Marcellus Shale-related samples, bulk shale sampled at depth and soil-mantled outcrop, that support the hypothesis that salts in flowback and production waters derive from brine in the Marcellus Shale itself.

Bulk samples of the Marcellus Shale were recovered from 850 to 874 ft (259 to 266 m) below land surface (bls) from core drilled near Howard, Pennsylvania, from one of the producing members (Union Springs Member of the Marcellus Shale). Samples were ground to <150 microns and digested using Li metaborate fusion prior to bulk elemental analysis. Separate splits of each sample type were also analyzed for $^{87}Sr/^{89}Sr$ using a Thermo Scientific Neptune Plus multiple collector inductively coupled plasma mass spectrometer (MC-ICP-MS). If the brine is present as free or capillary-bound water in the shale initially, much of the salt in brine is likely retained even after grinding because of the low permeability ($10^{-22}$ to $5 \times 10^{-20}$ m$^2$ ($10^{-10}$ to $5 \times 10^{-8}$ darcys) (Neuzil, 1994; King, 2012), grain size (see Figure 2), and low water saturation (Engelder, 2012). We investigated whether films of brine can be released during aqueous extraction for 12 h. The µmol per gram of shale of each element that was released by mixing with 20 ml (0.7 oz) distilled water (Table S1, Supplementary material available as AAPG Datashare 58 at www.aapg.org/datashare) was 0.02–0.03 Ba, 0.03–0.04 Sr, 3–5 Ca, 0.5–0.9 Mg, and 14–16 Na. Consistent with the presence of brine in the shale pores, mole leachate ratios (Mg/Na, Ca/Na, Mg/Ca, and Sr/Ba) are all within 30% of ratios reported for flowback waters from Pennsylvania (Hayes, 2009).

If brines are present in very fine pores in the Marcellus Shale, we might expect to see this brine

**TABLE 1.** Composition of Marcellus Formation Shale (core from Howard, Pennsylvania, near Bald Eagle State Park)

| Matrix Mineral | Formula | BE850[*] | | BE874[*] | |
|---|---|---|---|---|---|
| | | Mass % | Volume % | Mass % | Volume % |
| quartz | $SiO_2$ | 36.57 | 34.14 | 41.85 | 39.09 |
| albite | $NaAlSi_3O_8$ | 5.01 | 4.73 | 5.71 | 5.39 |
| calcite | $CaCO_3$ | 9.57 | 8.72 | 4.03 | 3.67 |
| illite | $KAl_3Si_3O_{10}(OH)_2$ | 28.83 | 25.5 | 29.7 | 25.98 |
| pyrite | $FeS_2$ | 5.48 | 2.7 | 5.54 | 2.74 |
| Mg-Fe chlorite[2†] | $(Mg_{0.6}Fe_{0.4})_{6-x}(Fe^{III}_{0.08}Al_{0.92})_x[Al_xSi_{4-x}O_{10}(OH)_8]$ | 10.35 | 8.87 | 9.13 | 7.81 |
| apatite | $Ca_5(PO_4)_3(OH, Cl)$ | 0.31 | 0.24 | 0.24 | 0.19 |
| SrO | SrO | 0.03 | – | 0.02 | – |
| BaO | BaO | 0.13 | – | 0.12 | – |
| MnO | MnO | 0.03 | – | 0.03 | – |
| $TiO_2$ | $TiO_2$ | 0.77 | – | 0.76 | – |
| organic matter | $C_nH_mO_l$ | 2.78 | 6.9 | 2.68 | 6.64 |
| salt/brine | | 0.14 | 2 | 0.19 | 2 |
| gas | $CH_4$ | – | 6.5 | – | 6.5 |

*Bald Eagle core, 850 or 874 ft (259 or 266 m) depth as indicated. This core was drilled in an overmature section of the Marcellus.
†$x = 2.3$ for BE850, and $x = 2.1$ for BE874.

salt even in surface outcrops of the Marcellus Shale. To investigate this, we examined both major and trace (Sr) elements in pore fluids sampled from a soil developed on the Marcellus Shale (Huntingdon, Pennsylvania; Mathur et al., 2012; Jin et al., 2013) and compared them with the geochemical compositions of production waters. The molar ratios (Mg/Na, Ca/Na, and Mg/Ca) differed between soil pore fluids and production waters, documenting that major elements in pore fluids are not dominated by brines if they are present. Such an observation could be explained by loss of much of the brine because of generation of porosity as shown in Figure 2. However, measurements on the soil developed on the Marcellus Shale documents that soil contains substantially more radiogenic Sr ($^{87}Sr/^{86}Sr$ equals ~0.750) than is contained in deeply sampled shale ($^{87}Sr/^{86}Sr$ equals~0.730), a difference that is consistent with weathering-induced loss of a less radiogenic, brine-derived Sr component originally present in the shale (see Datashare). In fact, the soil pore fluids are considerably less radiogenic (~0.730) than the coexisting soil (~0.750), suggesting the presence of an easily mobilized component in the soil, potentially brine trapped in

tight pores. It is not clear in what form or phase is the brine-derived Sr.

In summary, both the leachate elemental and $^{87}Sr/^{86}Sr$ analyses of Marcellus Shale support the hypothesis of a Na-Ca-Cl brine present in trace amounts in the shale at depth, which is consistent with the contention that the Sr content of flowback waters is partially controlled by reactions with radiogenic clays. With the leachate data, we then can utilize mixing calculations to determine how much salt is present. To calculate the geochemical composition of the bulk solid, we correct the measured solid geochemistry for the presence of leached elements, which are assumed to be added by pore brine, and recalculate elemental concentrations per gram of shale (Table 1). Using mineral data in Marcellus drill logs from 1950 to 2000 m (6398 to 6562 ft) depth (Engelder et al., 2014), we include quartz, illite, chlorite, calcite, and pyrite. To account for all the Na and P, we also included minor albite and apatite, common minerals in shales. The masses of leached elements were recast in terms of the masses of entrained brine salts: NaCl, KCl, $MgCl_2$, $CaCl_2$, $SrCl_2$, $BaCl_2$, and $Na_3PO_4$. Residual masses of one gram of shale not accounted for in the mass balance were assumed to be contained within organic matter (OM).

**TABLE 2.** Initial Total Salt Compositions of Injected Fracture Fluid and Pore Brine

| Chemical Entity | Injectate | Pore Brine (Well G) | Pore Brine (BE 850) | Pore Brine (BE 874) | Marcellus Shale Soil Water[*] |
|---|---|---|---|---|---|
| | | | Molality, mol $(kg\ water)^{-1}$ | | |
| $Li^+$ | – | $3.7 \times 10^{-2}$ | – | – | – |
| $Na^+$ | $1.58 \times 10^{-3}$ | 2.437 | 1.75 | 2.02 | $0.10 \pm 0.04$ |
| $K^+$ | $1.30 \times 10^{-4}$ | $1.34 \times 10^{-2}$ | $3.20 \times 10^{-1}$ | $5.14 \times 10^{-1}$ | $0.04 \pm 0.01$ |
| $Mg^{++}$ | $1.50 \times 10^{-4}$ | $5.74 \times 10^{-2}$ | $6.91 \times 10^{-2}$ | $1.21 \times 10^{-1}$ | $0.03 \pm 0.01$ |
| $Ca^{++}$ | $8.34 \times 10^{-4}$ | $6.223 \times 10^{-1}$ | $4.36 \times 10^{-1}$ | $6.42 \times 10^{-1}$ | $0.09 \pm 0.06$ |
| $Sr^{++}$ | – | $8.08 \times 10^{-2}$ | $4.57 \times 10^{-3}$ | $5.58 \times 10^{-3}$ | $0.0003 \pm 0.0001$ |
| $Ba^{++}$ | – | $6.99 \times 10^{-2}$ | $3.81 \times 10^{-3}$ | $2.41 \times 10^{-3}$ | $0.0007 \pm 0.0004$ |
| $Fe^{++}$ | $1.20 \times 10^{-5}$ | $1.01 \times 10^{-3}$ | – | – | – |
| $Cl^-$ | $2.46 \times 10^{-3}$ | 4.150 | 2.97 | 3.87 | $0.06 \pm 0.01$ |
| $SO_4^-$ | $6.10 \times 10^{-4}$ | $5.34 \times 10^{-4}$ | – | – | – |
| $PO_4^{3-}$ | – | – | $4.30 \times 10^{-2}$ | $6.89 \times 10^{-2}$ | – |
| | | | Elemental ratios (mol:mol) | | |
| $Mg^{++}/Na^+$ | | 0.024 | 0.040 | 0.060 | $0.3 \pm 0.1$ |
| $Ca^{++}/Na^+$ | | 0.26 | 0.25 | 0.32 | $1.0 \pm 0.6$ |
| $Mg^{++}/Ca^{++}$ | | 0.092 | 0.16 | 0.19 | $0.4 \pm 0.2$ |
| $Sr^{++}/Ba^{++}$ | | 1.2 | 1.2 | 2.3 | $0.6 \pm 0.3$ |

*Pore waters collected from deep soils (>40 cm depth, n = 12) developed on Marcellus Shale in the bottom of a hillslope position, Huntingdon County, Pennsylvania (Mathur et al., 2012; Jin et al., 2013).

The porosities of samples were set equal to ~8.5% as discussed above. Accordingly, minerals and organic matter occupy 91.5 vol. % of the shale volume. This volume ($V_{mins+OM}$) was calculated for 1 g (0.04 oz) of initial shale sample using the mineral composition (Table 1) and mineral densities, assuming the nominal density of OM is 1 g/cm$^3$ (62 lb/ft$^3$) (Schmoker, 1979, 1980, ). The 2% of the total shale volume was assumed brine filled. Using the calculated $V_{mins+OM}$, the volume filled by free or capillary-bound water can be calculated for 1 g (0.04 oz) sample: $2/91.5 \times V_{mins+OM}$. The resulting concentrations of salts in the brine were then recalculated to molality using the calculated brine density for the two samples (Table 2). These calculated concentrations compare favorably with brine compositions extrapolated from the time-series data reported for brine from ~2000 m (~6562 ft) depth in Lycoming County, Pennsylvania, noted here as Well G (Hayes, 2009). Although the density of OM may be as high as ~1.5 g/cm$^3$ (94 lb/ft$^3$) (Ward, 2010), such changes only increase brine concentrations by 3%.

The mole Sr/Ba ratio, which has been shown to be diagnostic of Marcellus brines, is similar in the leachate and the flowback brines (see example for Well G, Table 2). From a Sr isotopic perspective, brine-derived Sr in flowback has been observed to have higher $^{87}Sr/^{86}Sr$ ratios than marine evaporitic brines at depth in the Marcellus (i.e., Silurian brine from the Salina Formation; Chapman et al., 2012). This suggests a more radiogenic source of Sr in flowback waters, that is, Sr is derived from both radiogenic clays within the Marcellus Shale and the less radiogenic Silurian brines (~0.7083; McArthur and Howarth, 2004). This is consistent with previous suggestions that clay–water reactions contribute Sr to flowback and production waters (Chapman et al., 2012; Warner et al., 2012), as well as with our $^{87}Sr/^{86}Sr$ measurements of shale from Howard, Pennsylvania (0.730053 ± 0.00004 and 0.722974 ± 0.00004; Table 3). These deep core samples exhibit $^{87}Sr/^{86}Sr$ values that are more radiogenic than those reported for production waters from conventional wells in the Marcellus (i.e., 0.71000 to 0.71212; Warner et al., 2012).

## DIFFUSION MODEL

### Theoretical Background

Given that the shale may contain 1%–2% free or capillary-bound brine, we explore a mechanism to explain how flowback or production-water chemistry changes in salinity with time. In the model, diffusion of $N_p$ primary aqueous components through the porous rock matrix was described as

$$\phi \frac{\partial M_k}{\partial t} = \frac{\partial}{\partial x}\left(F_{inv}D^{aq}\frac{\partial M_k}{\partial x}\right) \qquad (1)$$

Here, $M_k$ is the molality of the $k$th component (i.e., salt) in the pore fluid ($k = 1, 2, …, N_p$), $\phi$ is the water-connected porosity in the matrix between fractures, $D^{aq}$ is the diffusion coefficient for species in the aqueous pore fluid, and $F_{inv}$ is the inverse of the Archie formation factor for the matrix (Archie, 1942; Brace, 1977; Balashov, 1995). The Archie formation factor takes into account the geometrical effects of pore connectivity, effective pore cross section, and pore tortuosity on diffusion through porous media.

Brine components are assumed to diffuse from the matrix into a set of planar subvertical hydrofractures of constant aperture (Figure 3) around a horizontal Marcellus wellbore. Because transport is faster in hydrofractures than through the matrix, concentrations in the fracture fluid are assumed constant everywhere. Thus, the problem of interest is the diffusion out of a planar porous sheet into a stirred solution of limited volume. Mathematically, this is the same problem as diffusion out of a stirred solution of limited volume into a planar sheet (Crank, 1980). Namely, if the solution of the original problem (Crank, 1980) is $M^{into}(x, t)$ and the solution of our problem is $M^{out}(x, t)$ then $M^{into}(x, t) + M^{out}(x, t)$ equals a constant.

The initial conditions for the diffusion problem are determined by (1) the composition of the dilute fracture injectate and (2) the composition of the brine, assumed to be in equilibrium with shale minerals (Table 2). Equilibration is expected given that brines have been present for millions of years in the shale. The spacing between fractures is $h_c$ (Figure 3). These equilibrium concentrations in the initial matrix

pore fluid are denoted as $M_k^{initial}$, $k = 1, 2, …, N_p$. Mass balance can be written for the interface of one fracture (Crank, 1980) as follows:

$$l_w \frac{dM_k^0}{dt} = -F_{inv}D^{aq}\frac{\partial M_k}{\partial x}\bigg|_{x=0} \qquad (2)$$

Here, the characteristic length scale is $l_w$, defined as half the fracture aperture ($w_c$). $M_k^0$ is the molality of the $k$th component ($k = 1, 2, …, N_p$) in the fracture solution (i.e., at $x = 0$) at time $t$. The characteristic time scale for such a diffusion problem is $l_w^2/F_{inv}D^{aq}$. Thus, equations 1 and 2 can be recast using the dimensionless space and time coordinates $\bar{x}$, $\bar{t}$ ($\bar{x} = x/l_w$, $\bar{t} = (F_{inv}D^{aq}/l_w^2)t$):

$$\varphi \frac{\partial M_k}{\partial \bar{t}} = \frac{\partial^2 M_k}{\partial \bar{x}^2}, \quad \frac{dM_k^0}{d\bar{t}} = -\frac{\partial M_k}{\partial \bar{x}}\bigg|_{\bar{x}=0} \qquad (3)$$
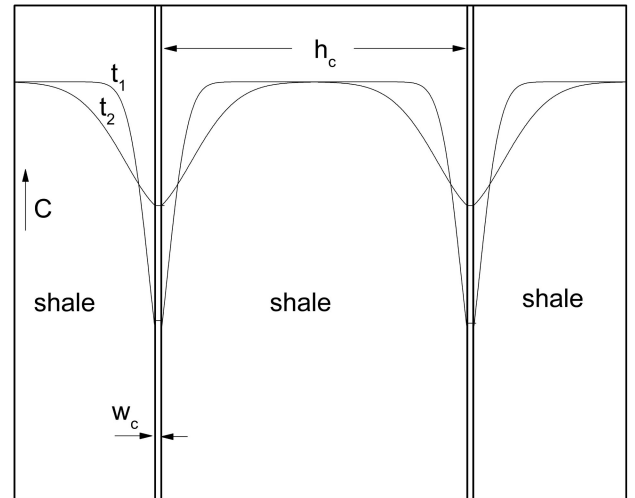


**Figure 3.** Schematic showing our model in which salt concentration C (plotted increasing upward on y axis) varies with position along a horizontal wellbore drilled through the Marcellus Shale (x axis; unfractured matrix is labelled shale). Two subvertical hydraulic fractures of aperture $w_c$ separated by distance $h_c$ are shown cutting through the shale. Prior to fracturing, the salt concentration in the pore fluid was assumed to be constant everywhere and equal to the values documented far from the fractures as shown by curves $t_1$ and $t_2$. In the model, it is assumed that the vertical fractures containing dilute water were emplaced at time 0. At $t = 0$ (not plotted), the profiles of salt concentration in the shale matrix would appear as horizontal lines that drop to 0 at the fracture walls. By time $t_1$, salt has diffused from the matrix into the fractures driven by the gradient in concentration of salt from the shale matrix to fracture. At $t_2 > t_1$, the salt concentration in the fracture has increased as shown.

The numerical solution for $M_k^0$ ($k = 1, 2, ..., N_p$) can be expressed as

$$M_k^0 = \frac{M_k^{\text{initial}}}{1 + \alpha} \varphi(\bar{t}) \qquad (4)$$

in which $\varphi(\bar{t})$ is a function of one variable ($\bar{t}$). As $\bar{t} \to \infty$, $\varphi(\bar{t}) \to 1$ and, correspondingly, $M_k^0 \to M_k^{\text{initial}}/(1 + \alpha)$. $M_k^{\text{initial}}$ is the initial salt concentration in the pore brine everywhere in the shale, and $\alpha$ stands for the ratio of the relative volume of hydrofractures ($\phi_d = w_c/h_c$) compared to the shale porosity $\phi$:

$$\alpha = \frac{w_c}{h_c \phi} = \frac{\phi_d}{\phi} \qquad (5)$$

The term ($\phi_d = w_c/h_c$) is described here as the hydraulic dilatancy. $\alpha$ is a small number on the order of ~0.01. For any porosity $\phi$, $\varphi(\bar{t})$ in equation (4) is a unique function of time. Furthermore, rescaling this function to real time is solely determined by one coefficient, $b_1 = F_{\text{inv}} D^{aq}/l_w^2$.

## Computation of Salt Diffusion into the Fracture

In all calculations, the temperature and pressure were set to 75°C (167°F) and 30 Mpa (4350 psi), that is, a shale layer at ~2 km (~6562 ft) depth and a geothermal gradient of 25°C (77°F)/km. Microseismic data from hydrofractured wells yields an idea of the stimulated reservoir volume (Edwards et al., 2011; Fisher, 2010). To a first-order approximation, hydrofracturing around a horizontal borehole of length $1.1 \times 10^3$ m (3609 ft) located in a well field with one horizontal bore every 300 m (984 ft) in the Marcellus will result in a stimulated layer of shale 45 m (148 ft) in the vertical dimension and 300 m (984 ft) in the horizontal dimension. Thus, the total volume of shale accessed per well ($V_a$) is approximately $1.5 \times 10^7$ m³ (~530 million ft³). We use this approximation as an upper limit for the stimulated volume per well. If the water volume ($V_u$) used for hydrofracturing is known, then the hydraulic dilatancy is $\phi_d = V_u/V_a$.

Any specific solution $M_k^0(t)$ of the diffusion problem can be represented in general form

(equation 4) using dimensionless $\bar{t}$ and can be used to determine $\varphi(\bar{t})$. The diffusion problem was solved using the numerical program MK76 (Balashov et al., 2013) for planar fractures of 0.64 mm (0.03 in.) aperture assuming 1 fracture per meter ($h_c = 1$ m) (0.3 fracture per foot) for a shale layer with matrix porosity ($\phi$) equal to 0.02. This specific problem corresponds to $\alpha$ equal to $0.643 \times 10^{-3}/0.02 = 0.032$. The mineral composition of the matrix was set to that summarized in Table 1, and the initial chemical compositions of the injectate water (Table 2) were set to dilute freshwater (Haluszczak et al., 2012). The initial chemical composition of the free or capillary-bound brine (Table 2; Table S2, supplement available as AAPG Datashare 58 at www.aapg.org/datashare) was set equal to pore brine extrapolated from the data of flowback chemistry for well G summarized in Table S2 (supplement available as AAPG Datashare 58 at www.aapg.org/datashare) (Hayes, 2009). Na, Mg, Ca, Cl, and $SO_4$ were included in the brine. For simplicity, the minor element Li was replaced by Na on a charge-equivalent basis, whereas Sr, Ba, and Br were replaced by Ca and Cl on a mole basis. Chemical equilibrium between brine and the shale mineral matrix was calculated using standard thermodynamic data (Balashov et al., 2013), resulting in a brine composition at depth as shown in Table S2 (supplement available as AAPG Datashare 58 at www.aapg.org/datashare).

Typical permeabilities range from $10^{-22} - 5 \times 10^{-20}$ m² ($10^{-7}$ to $5 \times 10^{-5}$ mD) for low-porosity (<10%) shales (King, 2012; Neuzil, 1994). The ratio of the permeability to the inverse Archie factor for rocks of low porosity is $K/F_{\text{inv}} \approx 10^{-17}$ m² (Zaraisky and Balashov, 1995). This yields an estimate for $F_{\text{inv}}$ in the range of $10^{-5} - 5 \times 10^{-3}$. For calculations here, the inverse Archie factor of the matrix ($F_{\text{inv}}$) was set to $1.8 \times 10^{-3}$.

The diffusion coefficients for chloride salts in aqueous solutions are observed to be equal within +20% (Robinson and Stokes, 1959). Here, the average salt diffusion coefficient ($D^{aq}$) was therefore set equal to $3.8 \times 10^{-9}$ m² s⁻¹ (Balashov et al., 2013).

Profiles of salt concentration in matrix pore fluid versus distance from fractures for the main aqueous components inside the shale were calculated as a function of time after injection (Supplementary

**TABLE 3.** The Results of Model Fitting

| Horizontal Wells | C | D | E | F | G |
|---|---|---|---|---|---|
| Used water volume ($V_u$), m³ | $17.434 \times 10^3$ | $2.521 \times 10^3$ | $6.379 \times 10^3$ | $9.299 \times 10^3$ | $14.775 \times 10^3$ |
| Hydrofracturing dilatancy ($\phi_d \times 100$), % | 0.11 | 0.016 | 0.042 | 0.061 | 0.096 |
| Fitted initial pore brine concentration ($M_k^0$ Vw⁻¹), kg m⁻³ | 350 | 152 | 368 | 208 | 261 |
| Fitted $b_1$, s⁻¹ | $1.01 \times 10^{-5}$ | $1.76 \times 10^{-5}$ | $1.09 \times 10^{-5}$ | $2.37 \times 10^{-5}$ | $6.94 \times 10^{-5}$ |
| Coefficient $b_2$, m² | $3.74 \times 10^{-4}$ | $2.14 \times 10^{-4}$ | $3.44 \times 10^{-4}$ | $1.59 \times 10^{-4}$ | $5.43 \times 10^{-5}$ |

material available as AAPG Datashare 58 at www. aapg.org/datashare).

This numerical solution was compared to an approximate analytical solution (Crank, 1980) for solution of equation 3, that is, the case of diffusion between a limited stirred volume (here, the hydrofracture volume) and a porous layer of infinite thickness (here, the shale matrix):

$$M_k^0 = M_k^{in}\left[1 - e^{\phi \bar{t}}\text{erfc}\left(\sqrt{\phi \bar{t}}\right)\right] \qquad (6)$$

A comparison of equation 6 with our numerical solution shows that the two solutions are practically identical over the applicable range of $\bar{t}$ (Figure S1, supplement available as AAPG Datashare 58 at www.aapg.org/datashare).

## Fitting the Diffusion Model to Field Data

The diffusion model was compared to the observed variation in total dissolved solids (TDS) shown in Figure 1 for flowback or production waters for five wells (Hayes, 2009; Haluszczak et al., 2012). The numerical solution (equation 4) for the system of equations (equation 3) was fit to the data by varying the scaling coefficient $b_1$ and the initial pore brine concentration, $\sum M_k^{initial}/V^w = \text{TDS}^{initial}$, using the Marquardt–Levenberg method. The results of fits are represented in Figure 1 and Table 3, and at higher time resolution in Figure S3, Datashare 58.

Using the fitted values of TDS$^{initial}$, a brine content of 2% by volume of the shale, and the estimated stimulated shale volume ($V_a$), the mass balance calculations show that only 0.1–0.2% of the salt in the initial brine accessed per well need be mobilized to explain the salt recovered at the surface.

If the $D^{aq}$ is known, it is convenient to calculate a new parameter, $b_2$: $b_2 = D^{aq}/b_1 = l_w^2/F_{inv}$ (in m²; Table 3) and then write

$$\log w_c = \frac{1}{2}\log F_{inv} + \log 2\sqrt{b_2} \qquad (7)$$

Equation 7 demonstrates that, for any given value of $D^{aq}$, the fitting coefficient $b_2$ places a constraint on fracture aperture ($w_c$) and the inverse Archie's formation factor ($F_{inv}$). Figure 4 shows a plot of equation 7 for model fits for the five wells from Figure 1. In this comparison, we implicitly assume that, in the model, the hydraulic fractures were filled by brine equivalent to the flowback chemistry that was reported at the land surface at any given time. In other words, the brine was assumed to flow instantaneously from depth to the land surface. The model therefore does not take into account that after some time the fractures would be filled by two phases: aqueous fluid and gas. Thus, the model likely underestimates the average fracture aperture at any given value of the inverse Archie formation factor, because it does not consider the fracture volume filled by gas. However, with more data, the diffusion model in principle could be updated to consider two-phase flow that would then be used to fit the time-series well data for both gas and water flow. The model nonetheless provides a useful first approximation of the dynamics of brine chemistry evolution with time.

In our model, we have implicitly assumed that gas mostly occupies the hydrophobic pores in organic matter (~ 6.5 vol. %) and that the brine is initially free or capillary bound in the ~ 2 vol. % of the rock that comprises hydrophilic pores (Gu et al., 2014). Thus, in our model the migration pathways of gas and brine from shale into the hydraulic fractures are different.
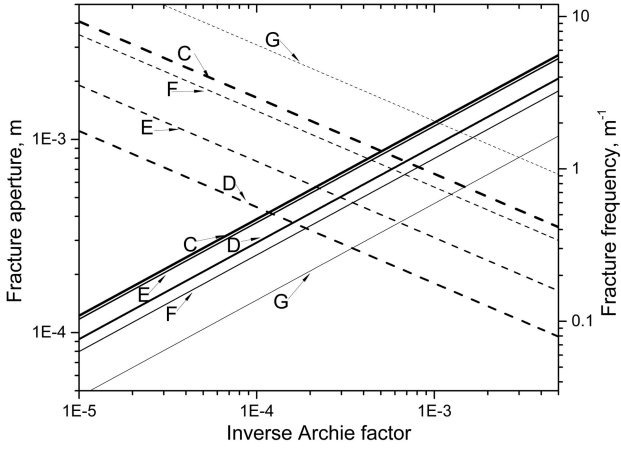
**Figure 4.** Plots of equations 7 and 11 using the values of $b_2$ derived for wells by the fits shown in Figure 1 (letter labels indicate well names). Solid lines denote fracture aperture (left axis) and dashed lines denote # fractures per meter (right axis), both plotted as a function of the assumed value of the inverse Archie factor $F^{inv}$. Lines derive from the fits of the model to the total dissolved solids data in Figure 1 for flowback and production water from five horizontal wells (C, D, E, F, and G; Hayes, 2009). The number of fractures per meter depends strongly upon the estimate of the stimulated volume of the shale for the horizontal well: this volume was in turn only constrained by micro-seismic data. For reasonable values of $F_{inv}$, the fracture aperture varies between tenths of millimeters and millimeters and the spacing varies between 0.2 and 5 m (0.7 and 16 ft).

However, some shale pores can accommodate both gas and brine. These pores will be able to support two-phase flow from shale into hydraulic fractures. To take account of this transport, the model would need to incorporate an advective term. For example, the hypothetical advective average flow $v$ during the first two weeks corresponding to our diffusion model could be expressed as

$$v \propto \frac{D^{aq} F_{inv}}{h} \tag{8}$$

in which $h$ is the distance of brine depletion in the shale measured in the direction orthogonal to the fracture plane after two weeks of recovery of flowback at the land surface. The model yields $h \propto 0.05$ m (2 in.) (Figure S2, Datashare 58). Estimating shale permeability ($K$) as $10^{-20}$ m$^2$ ($10^{-5}$ mD) and taking brine viscosity ($\eta_{br}$) equal to $5.2 \times 10^{-4}$ Pa s (Balashov et al., 2013), we can calculate the pressure gradient that would be necessary to produce the same advective

mass transfer as the previously calculated diffusion flux in our model during the first two weeks:

$$\nabla p_h \propto \frac{v\eta_{br}}{K} \approx 7 \text{ MPa m}^{-1} \tag{9}$$

This fluid pressure gradient is very high. Such a value probably can only be achieved in close vicinity to the horizontal bore during the first seconds or minutes of gas production. This simple quantitative estimation shows that salt diffusion from shale into hydraulic fractures will dominate over advective transfer under realistic fluid-pressure gradients. Documenting that the diffusion model is reasonable, we also show the good fit of the model to the data for the five horizontally drilled and hydrofractured wells (Hayes, 2009) in Figure 1 and Figure S3 (supplement available as AAPG Datashare 58 at www.aapg.org/datashare).

We can also use the hydraulic dilatancy calculated for planar fractures $\phi_d (= w_c/h_c)$, in which $h_c$ equals fracture spacing (m), to calculate the frequency of hydraulic fractures. Again estimating the dilatancy of the shale caused by hydraulic fracturing ($\phi_d$) from $V_a$ (the accessible volume of shale for one horizontal wellbore) and the water volume used for hydraulic fracturing, $V_u$ (Table 3) as $\phi_d = V_u/V_a$, we calculate the frequency of hydraulic fractures (m$^{-1}$) as $f_c = h_c^{-1} = \phi_d w_c^{-1}$. This leads to an expression for the fracture aperture:

$$w_c = \phi_d f_c^{-1} \tag{10}$$

Substituting equation 10 into equation 7, we derive the frequency of fractures, $f_c$:

$$\log f_c = -\frac{1}{2} \log F_{inv} + \log \frac{\phi_d}{2\sqrt{b_2}} \tag{11}$$

Five dashed lines corresponding to this equation are plotted in Figure 4 for the values of $b_2$ fit to each of the five wells (frequency labeled on the right axis). For reasonable values of $F_{inv}$, the fracture aperture varies between tenths of millimeters and millimeters, and the spacing varies between 0.2 and 5 m (0.7 and 16 ft). These five lines are highly dependent, however, on the assumed value of the stimulated volume ($V_a$). The $V_a$ is only poorly known and in our case is constrained only by the micro-seismic upper

limit. Nonetheless, the flowback chemistry can be used with the model to map out general characteristics of the structure of hydraulic fractures around a well.

## CONCLUSIONS

We have presented a reasonable quantitative model to explain important puzzles concerning the chemistry of flowback water from horizontal wells drilled in black shale. Specifically, we have addressed the questions of (1) where does the salt come from, and (2) why do salt concentrations increase in flowback and production water with time? We show that even with very low free-water content and ~2% by volume free or capillary-bound water in the shale prior to hydraulic fracturing, if this water has salt concentrations equivalent to Appalachian basin brines, then the total brine salt in the shale can explain the salinity of the produced waters. Indeed, extractions from the shale are consistent with 2% free or capillary-bound brine in the matrix. Nonetheless, bound water is not free to flow upward and out of the Marcellus: Our model is consistent with diffusion of salt from brine into mobile hydraulic fracturing water. This brine is present in core samples from depth but, as expected, is not present in exhumed outcrop shale samples that have higher porosity because of exhumation, except perhaps in  very small quantities that can only be detected by Sr isotope measurements. Using data from five wells and our diffusion transport model, changes over time are consistent with diffusion of salt from the shale matrix to hydrofractures containing dilute injectate water. Diffusion of Na, Ca, Mg, and Cl from free or capillary-bound water in the matrix to fractures can explain observed temporal changes in flowback chemistry. The model argues for a time lag of approximately 12 months after opening of the well before salt concentrations reach 90%–95% of the steady-state values. For reasonable parameter $F_{inv}$ values, apertures of hydrofractures that range from tenths of millimeters to millimeters and spacing of hydrofractures between 0.2 and 5 m (0.7 and 16 ft) are consistent with our model.

The model presented here could be refined with additional data specific for each well to yield more specific fracture-aperture and spacing information. In fact, if the model could be validated and parameterized more precisely, it might also be useful for predicting the concentrations and volumes of brine that will return to the surface in the future.

## REFERENCES CITED

Archie, G. E., 1942, The electrical resistivity log as an aid in determining some reservoir characteristics: Transactions of the American Institute of Mechanical Engineers, v. 146, p. 54–67.

Balashov, V. N., 1995, Diffusion of electrolytes in hydrothermal systems: Free solution and porous media, in K. I. Shmulovich, B. W. D. Yardley, and G. G. Gonchar, eds., Fluids in Crust: Equilibrium and Transport Properties: London, Chapman & Hall, p. 215–251.

Balashov, V. N., G. D. Guthrie, J. A. Hakala, C. L. Lopano, J. D. Rimstidt, and S. L. Brantley, 2013, Predictive modeling of $CO_2$ sequestration in deep saline sandstone reservoirs: Impacts of geochemical kinetics: Applied Geochemistry, v. 30, p. 41–56, doi:10.1016/j.apgeochem.2012.08.016.

Blauch, M. E., R. R. Myers, T. R. Moore, B. A. Lipinski, and N. A. Houston, 2009, Marcellus Shale post-frac flowback waters: Where is all the salt coming from and what are the implications?: SPE Paper, 125740, 20 p., doi:10.2118/125740-MS.

Brace, W. F., 1977, Permeability from resistivity and pore shape: Journal of Geophysical Research, v. 82, no. 23, p. 3343–3349, doi:10.1029/JB082i023p03343.

Brantley, S. L., D. A. Yoxtheimer, S. Arjmand, P. Grieve, R. D. Vidic, J. Pollak, G. T. Llewellyn, J. D. Abad, and C. Simon, 2014, Water resource impacts during unconventional shale gas development: The Pennsylvania Experience: International Journal of Coal Geology, v. 126, p. 140–156, doi:10.1016/j.coal.2013.12.017.

Chapman, E. C., R. C. Capo, B. W. Stewart, C. S. Kirby, R. W. Hammack, K. T. Schoroeder, and H. M. Edenborn, 2012, Geochemical and strontium isotope characterization of produced waters from Marcellus Shale natural gas extraction: Environmental Science and Technology, v. 46, p. 3545–3553, doi:10.1021/es204005g.

Crank, J., 1980, The Mathematics of Diffusion: Oxford, Oxford University Press, 432 p.

Dresel, P. E., and A. W. Rose, 2010, Chemistry and origin of oil and gas well brines in western Pennsylvania: Pennsylvania Geological Survey, 48 p.

Edwards, K. L., S. Weissert, J. Jackson, and D. Marcotte, 2011, Marcellus Shale hydraulic fracturing and optimal well spacing to maximize recovery and control costs: SPE Paper 140463, 13 p., doi:10.2118/140463-MS

Engelder, T., 2009, Marcellus 2008: Report card on the breakout year for gas production in the Appalachian Basin: Fort Worth Basin Oil and Gas Magazine, v. 20, p. 18–22.

Engelder, T., 2012, Capillary tension and imbibition sequester frack fluid in Marcellus gas shale: Proceedings of the National Academy of Sciences, v. 109, p. E3625.

Engelder, T., L. M. Cathles, and L. T. Bryndzia, 2014, The fate of residual treatment water in gas shale: The Journal of Unconventional Oil and Gas Resources, v. 7, p. 33–48.

Entrekin, S., M. Evans-White, B. Johnson, and E. Hagenbuch, 2011, Rapid expansion of natural gas development poses a threat to surface waters: Frontiers in Ecology and the Environment, v. 9, p. 503–511, doi:10.1890/110053.

Fisher, K., 2010, Data confirm safety of well fracturing: The American Oil & Gas Reporter, July.

Fjar, E., R. M. Holt, P. Horsrud, A. M. Raaen, and R. Risnes, 2008, Petroleum Related Rock Mechanics, 2nd ed., Amsterdam, The Netherlands: Oxford, UK, Elsevier, 491 p.

Gregory, K. B., R. D. Vidic, and D. A. Dzombak, 2011, Water management challenges associated with the production of shale gas by hydraulic fracturing: Elements, v. 7, no. 3, p. 181–186, doi:10.2113/gselements.7.3.181.

Gu, X., D. R. Cole, G. Rother, D. F. R. Mildner, and S. L. Brantley, 2014, Pores in Marcellus Shale: A neutron scattering and FIB-SEM study: Energy & Fuels, submitted.

Haluszczak, L. O., A. W. Rose, and L. R. Kump, 2013, Geochemical evaluation of flowback and production waters from Marcellus gas wells in Pennsylvania, USA: Applied Geochemistry, v. 28, p. 55–61.

Harper, J. A., 2008, The Marcellus Shale: An old "new" gas reservoir in Pennsylvania: Pennsylvania Geology, v. 38, p. 2–13.

Hayes, T., 2009, Sampling and analysis of water streams associated with the development of Marcellus shale gas, Marcellus Shale coalition: Des Plaines, Illinois, Gas Technology Institute, 80 p., www.bucknell.edu/MarcellusShaleDatabase.

Jin, L., R. Mathur, G. Rother, D. Cole, E. Bazilivskaya, J. Williams, A. Carone, and S. Brantley, 2013, Evolution of porosity and geochemistry in Marcellus Formation black shale during weathering: Chemical Geology, v. 356, p. 50–63, doi:10.1016/j.chemgeo.2013.07.012.

King, G. E., 2012, Hydraulic fracturing 101: What every representative, environmentalist, regulator, reporter, investor, university researcher, neighbor and engineer should know about estimating frac risk and improving frac performance in unconventional gas and oil wells: SPE Paper 152596, 80 p., doi:10.2118/152596-MS.

Maloney, K. O., and D. A. Yoxtheimer, 2012, Production and disposal of waste materials from gas and oil extraction from the Marcellus shale play in Pennsylvania: Environmental Practice, v. 14, p. 278–287, doi:10.10170S146604661200035X.

Mathur, R., L. Jin, V. Prush, J. Paul, C. Ebersole, A. Fornadel, J. Z. Williams, and S. L. Brantley, 2012, Cu isotopes and concentrations during weathering of black shale of the Marcellus Formation, Huntingdon County, Pennsylvania (USA): Chemical Geology, v. 304–305, p. 175–184, doi:10.1016/j.chemgeo.2012.02.015.

McArthur, J. M., and R. J. Howarth, 2004, Strontium isotope stratigraphy, in F. M. Gradstein, J. G. Ogg, and A. G. Smith, eds., Geological Timescale 2004: New York, Cambridge University Press, Cambridge, United Kingdom, p. 96–105.

MIT (Massachusetts Institute of Technology), 2011, The future of natural gas, http://mitei.edu/publications/reports-studies/future-natural-gas, Massachusetts Institute of Technology.

Neuzil, C. E., 1994, How permeable are clays and shales?: Water Resources Research, v. 30, no. 2, p. 145–150, doi:10.1029/93WR02930.

Nicot, J.-P., and B. R. Scanlon, 2012, Water use for shale-gas production in Texas, U.S.: Environmental Science and Technology, v. 46, p. 3580–3586, doi:10.1021/es204602t

Olmstead, S. M., L. A. Muehlenbachs, J.-S. Shih, Z. Chu, and A. J. Krupnick, 2013, Shale gas development impacts on surface water quality in Pennsylvania: Proceedings of the National Academy of Sciences, v. 110, no. 13, p. 4962–4967.

Osborn, S. G., A. Vengosh, N. R. Warner, and R. B. Jackson, 2011, Methane contamination of drinking water accompanying gas-well drilling and hydraulic fracturing: Proceedings of the National Academy of Sciences, v. 108, p. 8172–8176.

Poth, C. W., 1962, The occurrence of brine in western Pennsylvania: Pennsylvania Geological Survey Bulletin, v. M47, p. 1–53.

Robinson, R. A., and R. H. Stokes, 1959, Electrolyte Solutions: London, Butterworth Scientific, 646 p.

Rose, A. W., and P. E. Dresel, 1990, Deep brines in Pennsylvania, in S. K. Majumdar, E. W. Miller, and R. R. Parizek, eds., Water Resources in Pennsylvania: Availability, Quality and Management, Volume 12: Phillipsburg, New Jersey, The Pennsylvania Academy of Science Publications, p. 420–431.

Rowan, E. L., M. A. Engle, C. S. Kirby, and T. F. Kraemer, 2011, Radium content of oil- and gas-field produced waters in the northern Appalachian Basin (USA): Summary and discussion of data: Reston, Virginia, U.S. Geological Survey, 31 p.

Schmoker, J. W., 1979, Determination of organic content of Appalachian Devonian shales from formation density logs: AAPG Bulletin, v. 63, p. 1504–1537.

Schmoker, J. W., 1980, Determination of organic matter content of Appalachian Devonian shales from gamma ray logs: AAPG Bulletin, v. 64, p. 2156–2165.

Vidic, R. D., S. L. Brantley, J. M. Vandenbossche, D. A. Yoxtheimer, and J. D. Abad, 2013, Impact of shale gas development on regional water quality: Science, v. 340, p. 826, doi:10.1126/science.1235009.

Ward, J. A., 2010, Kerogen density in the Marcellus Shale: SPE Paper 131767, 4 p.

Warner, N. R., R. B. Jackson, T. H. Darrah, S. G. Osborn, A. Down, K. Zhao, A. White, and A. Vengosh, 2012, Geochemical evidence for possible natural migration of Marcellus Formation brine to shallow aquifers in Pennsylvania: Proceedings of the National Academy of Sciences, v. 109, p. 11,961–11,966.

Zaraisky, G. P., and V. N. Balashov, 1995, Thermal decompaction of rocks, p. 253–284, in K. I. Shmulovich, B. W. D. Yardley, and G. G. Gonchar, eds., Fluids in Crust: Equilibrium and Transport Properties: London, Chapman & Hall, p. 253–284.